



A submarine canyon conduit under typhoon conditions off Southern Taiwan

James T. Liu*, Hui-Ling Lin, Jia-Jang Hung

Institute of Marine Geology and Chemistry, National Sun Yat-sen University, Kaohsiung, Taiwan 804-24, Republic of China

Received 5 October 2004; received in revised form 19 July 2005; accepted 27 September 2005

Available online 28 November 2005

Abstract

The function of a submarine conduit under typhoon conditions is examined. The study site is the Kao-ping river, shelf, and submarine canyon (KPRSC) system located off southern Taiwan on a wave-dominated microtidal coast. The head of the canyon is located approximately 1 km off the river mouth. Two comprehensive 1-month field experiments were carried out in 2000 and 2002 during the flood season of the river. Both experiments encountered typhoons that generated significant river discharge and wave resuspension events. Particle samples collected in 2000 by sediment-traps were analyzed for coarse fraction by the wet sieving method. Among the coarse fraction, foraminiferal species and their abundance were recorded as a tracer for biogenic particles of marine origin. Stable isotopes of carbon ($\delta^{13}\text{C}$) of organic particles of sediment-trap samples were analyzed as a tracer for particles of terrestrial origin. All the measured flow and particle concentration records were analyzed by conventional time-series analytical methods. Simultaneously observed records of suspended sediment concentration at the river mouth and the volume concentration of suspended particles near the canyon floor were compared. Instantaneous flux and cumulative transport of suspended particles near the canyon floor were estimated during the deployment period. Results show that Kao-ping Submarine Canyon is a multi-level and process-dependant two-way conduit for particles of terrestrial and marine origins. In general, terrestrial signals are stronger than the marine signals in sediment-trap samples near the head of the canyon. During typhoon events, in the early distal phase of their influence nonlithogenic and biogenic marine sources are enhanced; in the later proximal phase signals of locally generated terrestrial lithogenic sources are enhanced. An episode of momentary downcanyon flushing of suspended particles near the canyon floor is observed during one typhoon occurrence. This flushing suggests nondeposition during the typhoon at the locale of deployment despite increased input of particles to the canyon floor. It also suggests a mechanism by which turbidity currents could be triggered. Yet, this flushing phenomenon is not observed in another typhoon occurrence, suggesting it is not universal in the canyon's response to the typhoon.

© 2005 Elsevier Ltd. All rights reserved.

Keywords: River-sea system; Submarine canyon; Particle size; Nonlithogenic source; Biogenic source; Typhoon; Sediment-trap; Taiwan

1. Introduction

Worldwide in many river-sea transport systems that include submarine canyons, storms and energetic weather events play an important role in the hydrodynamics and particle transport on the shelf

*Corresponding author. Fax: +886 7 525 5130.

E-mail address: james@mail.nsysu.edu.tw (J.T. Liu).

and in the canyon (Harris et al., 2003; Liu and Lin, 2004; Ogston et al., 2000; Puig and Palanques, 1998; Puig et al., 2003; Skliris et al., 2004). Usually the influence of storms is system-wide, affecting all aspects of material generation, delivery, transport, and deposition (Liu and Lin, 2004; Puig and Palanques, 1998; Wheatcroft, 2000).

High but episodic river discharge events often occur during storms, resulting in rapid delivery of river-borne sediment to the shelf and canyon (Liu et al., 2004; Ogston et al., 2000). During storms, higher wave energy mobilizes shelf substrate, leading to increased supply of shelf sediment to the submarine canyon (Liu et al., 2004). In some cases the coincidence of high river flood events and storm-related energetic wave regime facilitates the formation of fluid mud on the shelf, which is subsequently transported further by gravitational forcing (Fan et al., 2004; Ogston et al., 2000).

The heightened wind field during the storm increases the level of turbulent diffusion, which in turn increases the vertical mixing of the water column around the submarine canyon (Skliris et al., 2004). If the increased wind stress is also downwelling favorable, this will lead to homogenization of the water over the canyon (Sobarzo et al., 2001) and to downcanyon transport of coastal water towards the abyssal plain (Skliris et al., 2004). Near-bottom cross-shelf transport of particular matter could also be triggered by storm waves in the presence of downwelling-favorable winds (Vitorino et al., 2002).

During an energetic storm in the absence of a river flood event, high near bed suspended sediment concentration (SSC) was observed in the head region of Eel Canyon, which is associated with fluid mud, driven by density-driven flows (Puig et al., 2003). In the same event, inside the canyon, near-bed sediment fluxes were downcanyon. In the Hudson Shelf Valley, down-valley sediment transport is associated with storms that produce energetic waves and downwelling favorable winds (Harris et al., 2003). Shelf-slope sediment transport through Foix Canyon takes place sporadically during and immediately after an important storm event of a river discharge increase (Puig and Palanques, 1998).

The influence of storms is not restricted to the hydrodynamics and suspended sediment transport near the substrate-water interface. In stratigraphic records, fluid mud deposits are identified on the California shelf (Fan et al., 2004), which are

associated with storms. Turbiditic deposits in Capbreton Canyon are attributed to turbidity currents triggered by a violent storm (Mulder et al., 2001). Storms are also a possible cause for the observed turbidity currents in Monterey Canyon (Xu et al., 2004).

There is no doubt that in a river-sea transport system storms are agents not only for delivery of terrestrial sediments to the coastal seas and generation and transport of lithogenic and nonlithogenic particles on the shelf and inside the canyon; they are also responsible for strata formation on the shelf and in the canyon. All these processes influence the characteristics of the submarine conduit. However, not much is known about how storms affect the suspended particle dynamics in a submarine canyon on the event scale in which significant settling and transport occur. Furthermore, little attention has been paid to distinguishing the different source and modes of delivery of lithogenic and nonlithogenic particles during storm events. In this paper we present findings during two typhoon events from a river-shelf-canyon system located on the arc-continent collision belt between Taiwan orogen and Chinese continent margin (Liu et al., 1997). The focus of this paper is on how the submarine conduit functions under typhoon conditions.

2. Study area and background

Because of its tectonic and topographic setting, climate, and geographic location, the island of Taiwan is an ideal natural laboratory for studying the export of terrestrial substances (Dadson et al., 2003), their fate and their influence on the neighboring marginal seas (Hsu et al., 2004). The study site is the Kao-ping river, shelf, and submarine canyon system (KPRSC) located off southern Taiwan on a wave-dominated microtidal coast (Fig. 1). It is composed of three geographically separated dynamic entities: the river plume, the shelf, and the canyon (Liu and Lin, 2004). The Kao-ping River (KPR) is the largest river in Taiwan in terms of basin area and length. Because of the geology, topography, climate, and human activities in the river basin, both physical weathering and chemical weathering rates are significantly higher than the world average (Hung et al., 2004). On average, during the flood season (from June to September) the river discharge is 2–3 orders of magnitude, the sediment load is 2–3 orders of magnitude, and the

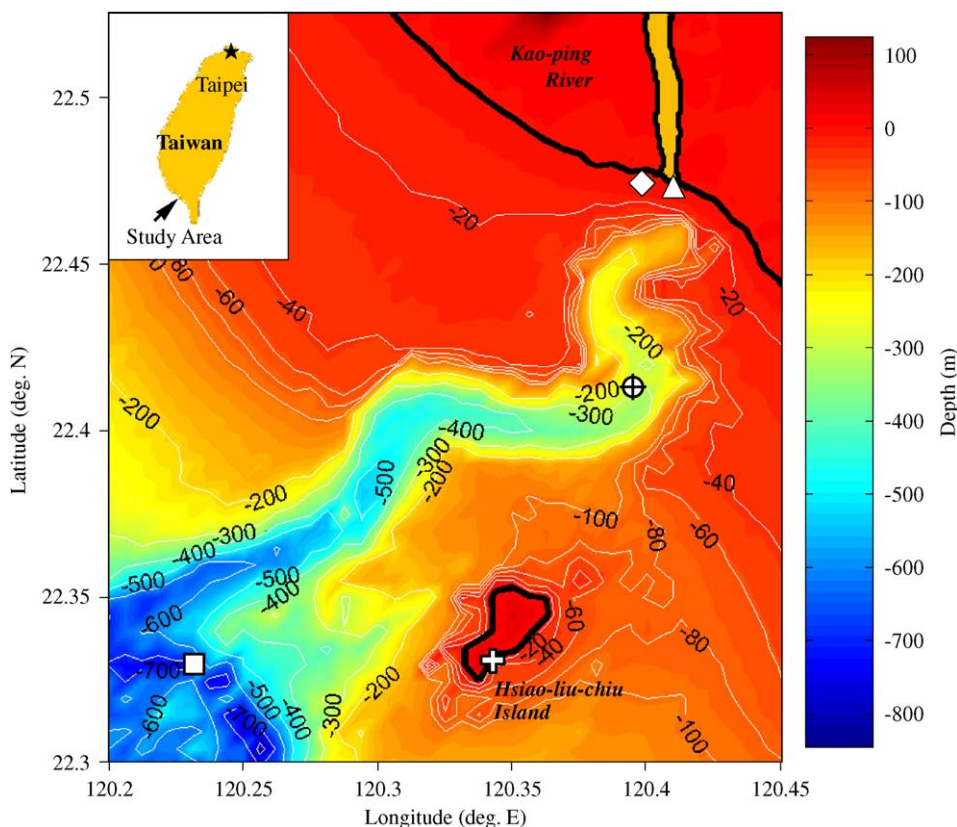


Fig. 1. Map shows the bathymetry of the study area and locations of moored tripod at the mouth of the Kao-ping River (triangle) and the sediment-trap array (circle with a cross). The open cross indicates the location of the weather station where the weather data was obtained. The square indicates the hydrographic station from which the measured T–S diagram is used for the reference of South China Sea water. Depth contours are in meters based on the Kee-lung mean sea level (data provided by the National Center for Ocean Research). The inset is a larger-scaled map of Taiwan.

sediment flux is 5 orders of magnitude greater than those in the dry season.

Under fair weather conditions for both dry and flood seasons of the river discharge, the river plume and the shelf are coupled mostly through the wind field and tidal flows. Dynamically, the submarine canyon is not closely coupled with the other two entities. Since the head of the submarine canyon is located immediately seaward of the river mouth, the river and submarine canyon form a direct sediment source-to-sink pathway for the coarse siliciclastic sediment (Liu et al., 2002; Liu and Lin, 2004). The shelf process plays only a secondary role in terms of source-generation and pathway (Liu and Lin, 2004).

The canyon is not only a conduit through which particles of terrestrial and marine origins pass back and forth in the course of a tidal cycle (Liu and Lin, 2004), it is also a sink (trap) in which the long-term sediment transport direction is upcanyon toward a

dead end (Liu et al., 2002). In a previous study, Liu and Lin (2004) focus only on the lithogenic aspect of the sediment sources for the canyon and find the canyon receives both terrestrial sediments discharged by the nearby Kao-ping River and lithogenic and biogenic sediments from the shelf. This paper is a continuation of the previous paper in which we present some nonlithogenic aspects of the particles that enter the submarine canyon in terms of their sources, transport, and especially their delivery during typhoon events; the documentation of a typhoon-related sediment-flushing event; and the differences between the impact of two typhoons and their implications.

3. Field experiments

Two comprehensive 1-month field experiments were carried out, in 2000 and 2002, during the flood

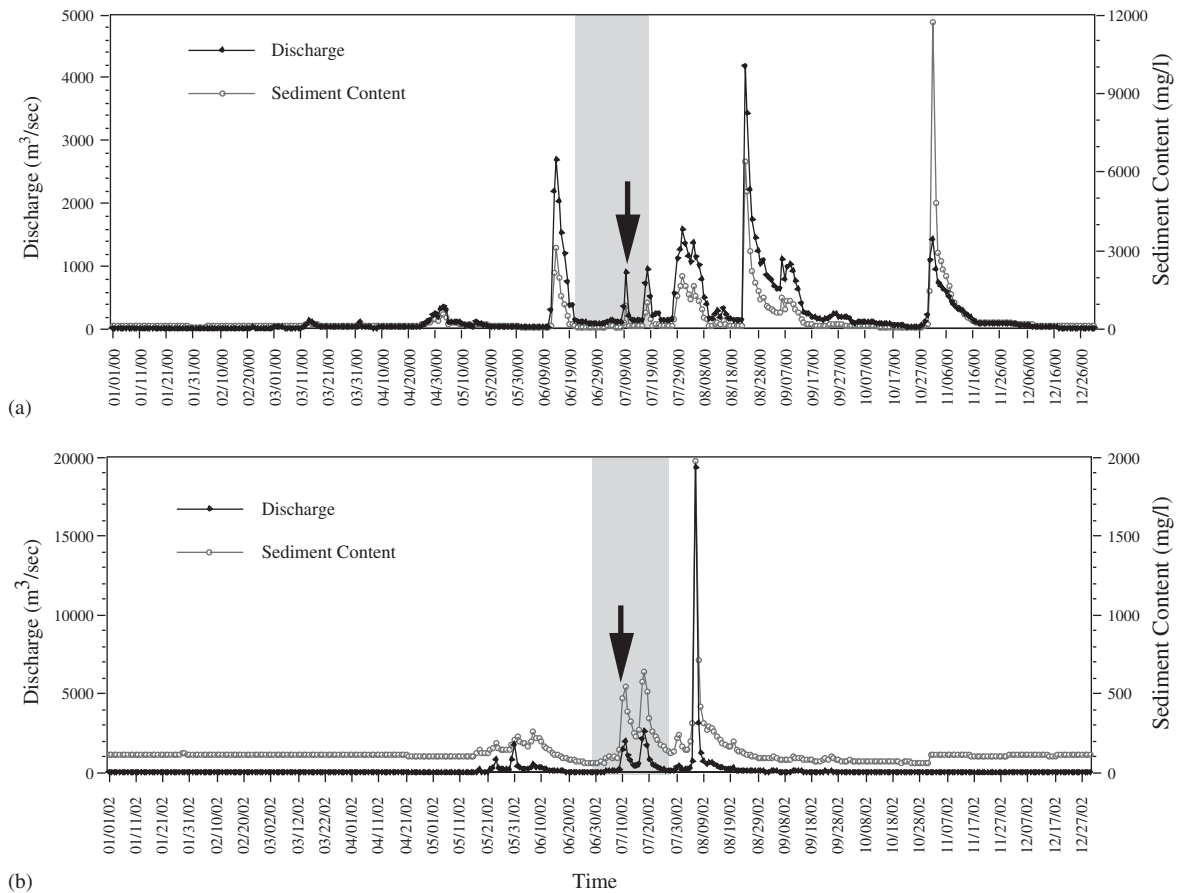


Fig. 2. Daily river discharge and suspended sediment concentration measured at the nearest gauging station (approximately 30 km) from the river mouth for the years 2000 (a) and 2002 (b). The shaded area indicates the duration of the one-month field experiment in each year. The two arrows point to two typhoon-related discharge events in both years. The Water Resources Bureau provided the discharge and suspended sediment content data.

season of the KPR (Fig. 2). Both experiments encountered typhoons that generated significant discharge events (Figs. 2 and 3). Detailed description of the typhoon event in 2000 has been given in Liu and Lin (2004); it will not be repeated here. In 2002, two typhoons occurred (Fig. 3), but only the second one, Typhoon Nakri, made detectable impact in the study area (Fig. 2(b)).

The deployment strategies for both experiments were similar, including an instrumented tripod located immediately seaward of the mouth of the KPR, an upward-looking ADCP on the shelf near the river mouth, and a two-level sediment-trap array in the submarine canyon (Liu and Lin, 2004).

3.1. Tripod

The tripod consisted of a directional wave, tide, and current gauge (SeaPac 2100) having an addi-

tional channel for an optical backscatterance sensor (OBS) and a CTD (TD-410). The EM current meter and the OBS of SeaPac 2100 were both positioned at approximately 1 m above the sea bed. However, in 2002 the CTD malfunctioned, and consequently salinity and temperature data were not available. During both deployments, water samples were taken at the tripod site at depths close to the OBS. These samples were later analyzed for SSC, which in turn were used to convert the OBS readings (FTU) to mg/l.

3.2. Upward-looking ADCP

One acoustic Doppler current profiler (ADCP) made by R&D Instruments (600 kHz work-horse having the bin size of 1 m) was deployed on the shelf not too far from the tripod site at a depth of about 15 m (Fig. 1). The sampling rate was

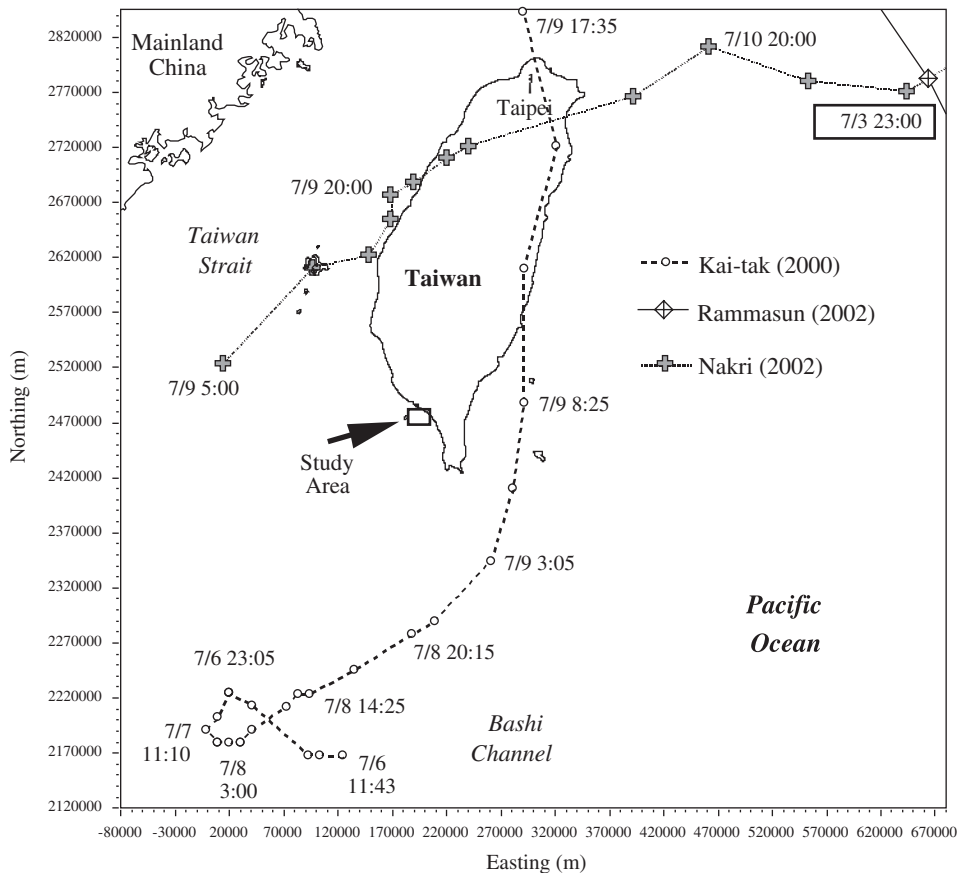


Fig. 3. The tracks of three typhoons around Taiwan encountered during the field experiments. Open circles represent Kai-tak in 2000, diamond represents Rammasun in 2002, and crosses represent Nakri in 2002. At discrete locations along the typhoon tracks, the time is annotated.

set at 10 min, and only the data points whose quality exceeded the criterion of '85% good' were used.

3.3. Taut-line sediment-trap array

The sediment-trap array with two levels of instrumentation was deployed from R/V Ocean Researcher III at similar locations (Fig. 1) on the seaward side of the convergence zone suggested by sediment transport vectors according to Liu et al. (2002). The water depths were approximately 290 m in 2000 and 313 m in 2002.

In 2002, the sediment-trap array was configured differently than in 2000 (Table 1, Liu and Lin, 2004) but used the same type of instruments. The upper level instrumentation set on the taut line, including LISST-100, cylindro-conical-shaped sediment-trap

with twelve 250 ml collecting cups (Technicap PPS 3/3 having aspect ratio of 2.5 and collecting area 0.125 m^2) and an RCM current meter was moved upward on the taut-line to be near the upper rim of the canyon instead of being in the lower part of the canyon. Unfortunately, the taut line was severed by unidentified means (sabotage was suspected) at a point about 18 days into the experiment. Consequently, the upper part of the array containing the upper level instrumentation set was missing at the time of retrieval. The breakup of the array caused insufficient floatation for the middle section of the array, resulting in downward tumbling of some of the instruments, which led to malfunctioning. The only two instruments that survived and remained functional were an RCM current meter at about 33 m above the sea bed (mab) and a LISST-100 at about 28 mab.

Table 1
Chronology of typhoon Kai-tak related events in 2000

Timeline	Event	Phase
08:00 7/4	1. Lowest point of F_t at upper trap (Fig. 7(b))	Distal
14:00 7/4	2. Peak values of particle sizer-analyzed coarse fraction at both levels (Fig. 8(a), Liu and Lin, 2004)	Distal
16:00 7/4	3. Peak values of sand-sized suspended particle flux near the canyon floor (Fig. 19b, Liu and Lin, 2004)	Distal
20:00 7/6	4. Lowest points of TOC for both traps (Fig. 6(a))	Distal
20:00 7/6	5. Peak values for planktonic and benthic foram concentrations at both levels (Fig. 6(b))	Distal
20:00 7/6	6. Peak values of wet-sieved coarse fraction at both levels (Fig. 8(b), Liu and Lin, 2004)	Proximal
02:00 7/7	7. Peak wave height on the shelf (Fig. 6(b))	Proximal
03:00 7/9	8. Lowest atm. pressure (Fig. 4(a), Liu and Lin, 2004)	Proximal
08:25 7/9	9. Shortest distance between the center of typhoon and the study area (Fig. 3)	Proximal
03:00 7/10	10. Abrupt change of local wind direction (Fig. 4(a), Liu and Lin, 2004)	Proximal
15:00 7/10	11. Peak value of daily river discharge and sediment content (Fig. 2(a))	Proximal

Note: The accuracy of each timeline is to the nearest tick mark on the corresponding figure.

4. Analyses of sediment-trap samples in year 2000

4.1. Foraminiferal abundance

Dry particles in the coarse (greater than 63 μm) fraction obtained from wet sieving were sieved again by 150 μm opening sieve. All foraminiferal shells, both planktonic and benthic, were then picked and identified from the portion greater than 150 μm . Concentrations of foraminiferal shells were calculated and expressed as number of individual shells per gram of dry sediment sample (#/g).

4.2. Total organic carbon content

Total organic carbon contents were measured with a LECO CS-224 carbon/sulfur analyzer. One aliquot of weighed sample was first digested with 3 N HCl to remove the carbonate phases (inorganic carbon). Sample was then cleaned with distilled water and weighed again after the organic carbon determinations. Analytical precision of the analyses is $\pm 0.02\%$.

4.3. Stable isotopes of carbon ($\delta^{13}\text{C}$) of organic particles and the estimate of mixing factor (F_t)

In the carbon isotopic analyses, about 50 mg of sediment-trap sample was used. To completely remove the carbonate, 2.0 M HCl was added to the samples at 55 $^\circ\text{C}$ under vacuum conditions. The preparation and purification of CO_2 from carbonate-free samples for isotopic analyses of organic carbon generally followed the methods of Craig (1953) and Sheu et al. (1995). The purified CO_2 gas was then analyzed with a VG Optima isotope

ratio mass spectrometer (IRMS). The precision of isotopic measurements through the analytical procedure was deemed better than $\pm 0.15\%$.

The carbon isotope $\delta^{13}\text{C}$ of organic particles captured by the sediment-trap array was seen as a tracer to indicate the extent of mixing (F_t) between terrestrial and marine end members, such that

$$\begin{aligned} \delta^{13}\text{C}(\text{measured in the canyon}) \\ = \delta^{13}\text{C}(\text{measured in the lower river}) \\ \times F_t + \delta^{13}\text{C}(\text{in marine diatom}) \times (1 - F_t). \quad (1) \end{aligned}$$

An average value of -25.86 was used to represent the terrestrial end member from the analysis of sediment samples taken from the lower part of the KPR. The value for the marine end member was assumed to be -19.5 from marine diatoms (Perterson and Howarth, 1987).

5. Results

5.1. Year 2000 experiment and typhoon Kai-tak

Some observations from the 2000 experiments have been described in detail by Liu and Lin (2004), they will not be repeated. Among the unreported observations, only data pertaining to this paper are presented herein.

5.1.1. Net water movements on the shelf and in the lower part of the canyon

The plot of progressive vectors of the near-surface (about 10 mab) and near-bottom (about 1.5 mab) flow shows that the flow field on the shelf was dominated by a northwesterly (shore-parallel) mean flow superimposed by tidal oscillations (Fig. 4(a)).

The flows measured concurrently at approximately 50 and 100 mab in the canyon show that although tidal motions at semidiurnal frequencies were dominant, the net movements were in opposite directions (Fig. 4(b)). At 100 mab, the net water flow was downcanyon (Fig. 4(a)). Near the canyon floor (50 mab), the net flow of water was upcanyon (Fig. 4(b)). Between June 26 and July 6 the upcanyon flow at 50 mab was accelerated which coincided with the neap-to-spring phase of the tide (Fig. 5(a)). During the spring-to-neap phase of the tide from July 6 to July 16, oscillatory tidal motions dominated the flow regime (Fig. 5(a)), and the net upcanyon movement was ‘stalled’ (Fig. 4(b)).

5.1.2. Mass fluxes

Among the 12 collection cups on each sediment trap, all except for the first 4 were filled to the rim (overflowing) at the time of retrieval. Liu and Lin

(2004) gave a detailed description on how the samples were analyzed for the mass fluxes but did not present the results. The data are shown in Fig. 5(b). Comparing with the flow measurements, the time of unfilled collecting cups coincided with the neap tide (Figs. 5(a) and (b)). During this time, the lower trap (54 mab) had higher mass fluxes than the upper trap (104 mab). As the tide moved from neap to spring, the observed mass fluxes increased from June 26 to July 2. The high tide signifies the beginning of the overflowing collecting cups through the remainder of the deployment, of which the estimated mass flux exceeds $700 \text{ g/m}^2/\text{day}$. This number is three orders of magnitude greater than the measured particulate fluxes in northeastern South China Sea (SCS) off southwest Taiwan (Chung et al., 2004). However, after the passing of spring tide, the measured mass fluxes remained no less than $700 \text{ g/m}^2/\text{day}$ until the end of the deployment.

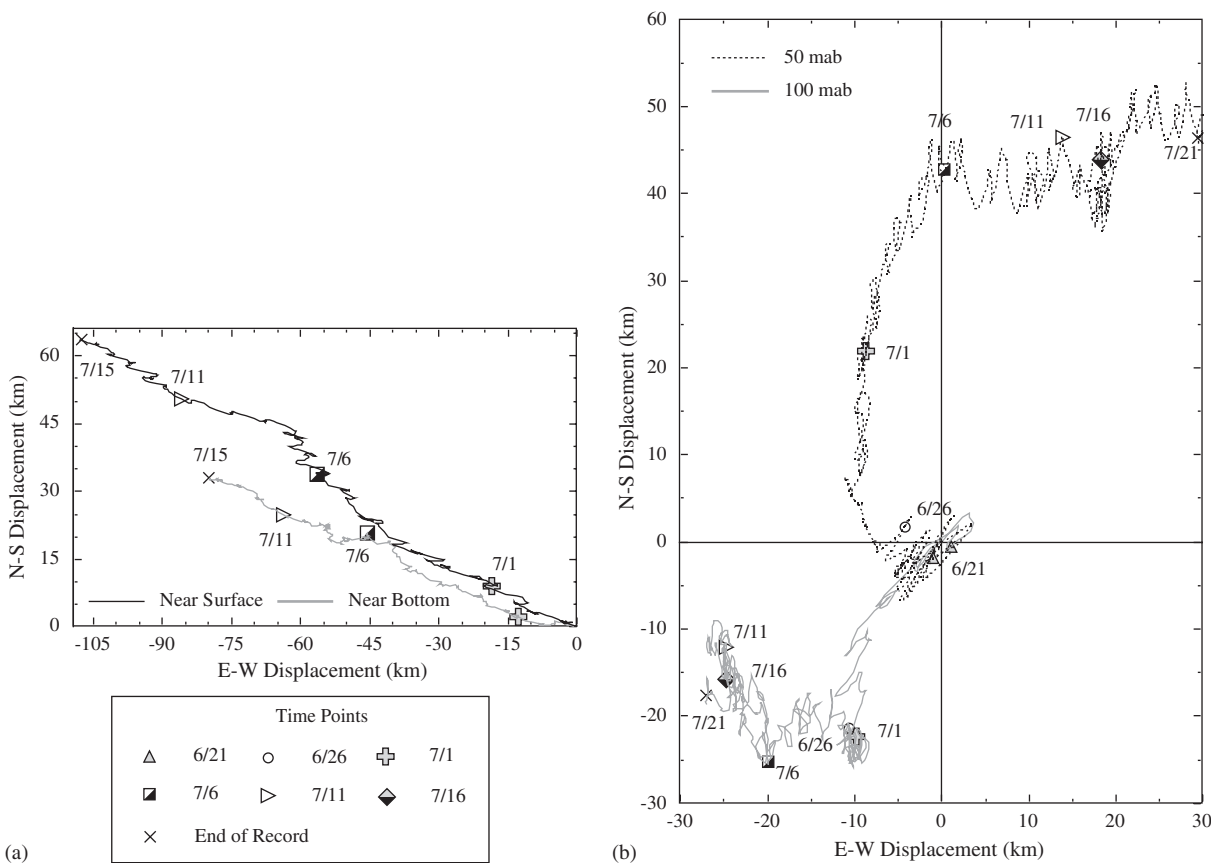


Fig. 4. Progressive vectors of (a) the near-surface and near-bottom flow on the shelf (from 16:00 June 29 to 18:00 July 15), and (b) the flow at approximately 50 and 100 mab in the canyon (from 15:00 June 20 to 13:00 July 21) in 2000. At discrete points in each time series the time is annotated. The origin in each plot is the beginning of the record and the ‘x’ marks the end of the record.

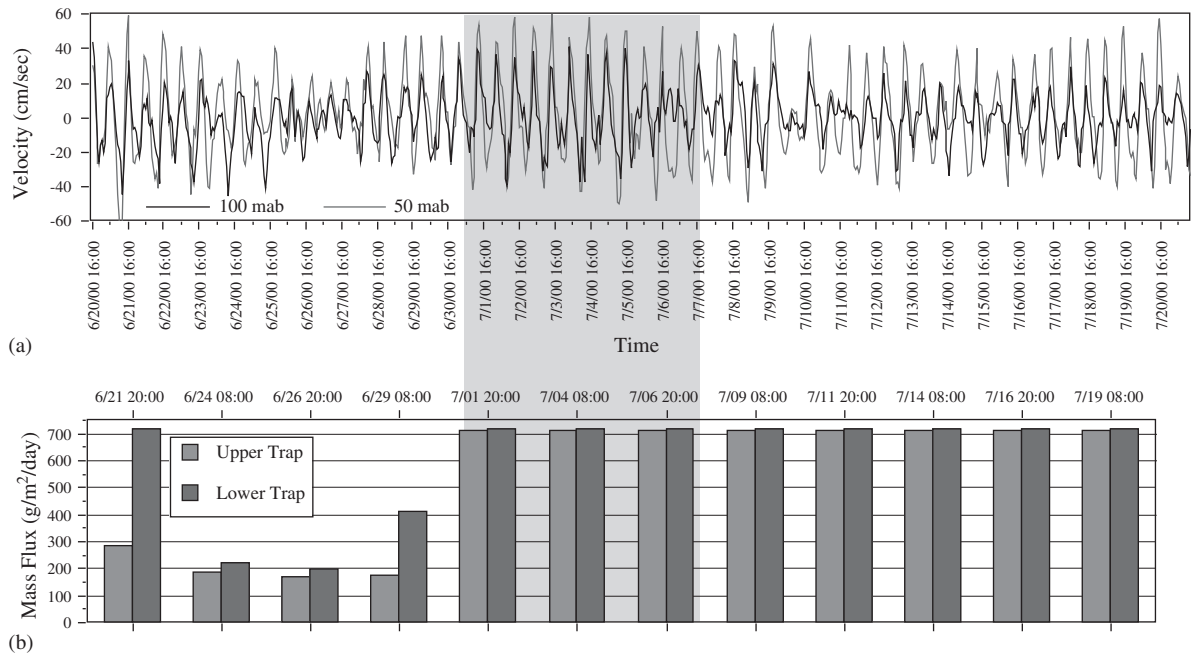


Fig. 5. Data from the sediment-trap array showing the time series of the along canyon component of the flow at 50 and 100 mab (a), and estimated mass fluxes (lower limits except first four cups) in the upper and lower traps (b). The shaded box indicates the period of spring tide.

5.1.3. TOC content

Liu and Lin (2004) point out the discrepancy in the abundance of the coarse fraction in the sediment-trap samples by the wet sieving method and laser particle analyzer method. Although they attribute this difference to the differential degree of preservation of nonlithogenic particles, their focus was on the lithogenic particles. They gave no further discussion on the nature of nonlithogenic particles is given.

The TOC content shows a period of low values corresponding to the passing of the typhoon, whose local influence is represented by the observed wave height (Fig. 6(a)). When high waves subsided, higher TOC values returned to pre-typhoon levels.

Under most sedimentary conditions, biogenic organic matter is relatively labile in comparison with other particles, including lithogenic and non-lithogenic, because of its sensitivity to oxidative degradation. Although there are many factors influencing the TOC content of marine sediments, recent modelling results suggest that 'preservation' surpasses 'dilution' when sedimentation rate is less than 5 cm/ky (Tyson, 2001). Sedimentation rates at our study area, however, are significantly greater than 5 cm/ky according to ²¹⁰Pb-determined values

(40 to greater than 150 cm/ky; Huh, unpublished data). During energetic typhoon events, the increased delivery of older particles would cause dilution of the TOC in the sediment-trap samples. These older particles came either by direct settling from the shelf above of reworked substrate or by lateral advection along the canyon by storm-related flow. Subsequently, during the typhoons lower values of TOC content are expected when mass fluxes increase.

5.1.4. Foraminiferal abundance

The abundance of both benthic and planktonic foraminifer species in terms of number of individuals per gram in the wet-sieved coarse fraction was recorded (Fig. 6(b)). The planktonic fauna consists mainly of *Globigerinoides bulloides*, *Globigerinoides aequilateralis*, *Globigerinoides ruber*, *Globigerinoides sacculifer*, and *Neogloboquadrina dutertrei*. The taxa of the benthic fauna included both shelf and bathyal species (Lin et al., in press). The influence of the typhoon is clearly seen in the abrupt increase of the foraminiferal abundance for both the planktonic and benthic species in collecting cups at both levels centered at the time 20:00 on July 6. The abundance at the two levels displays different

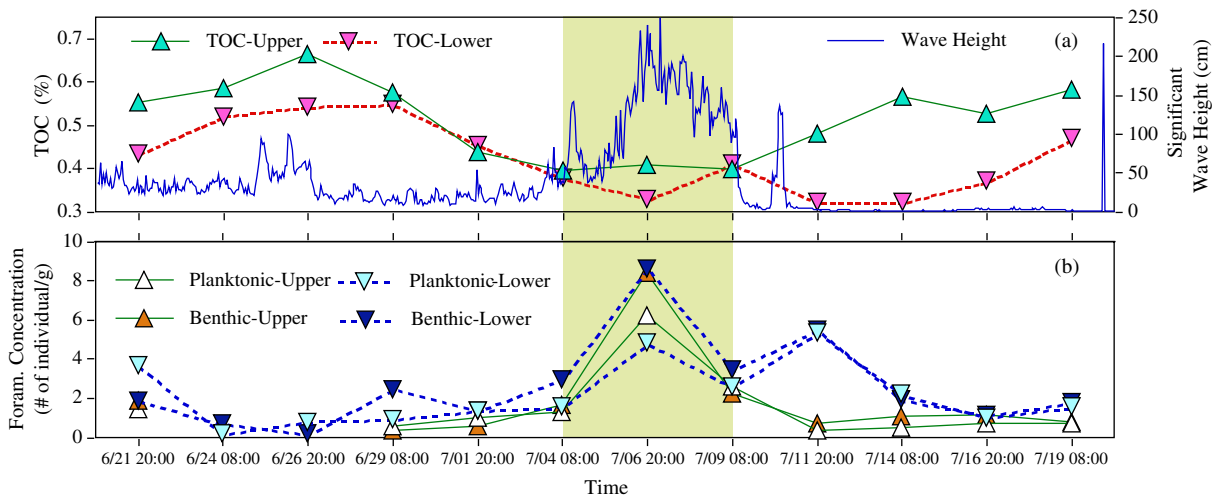


Fig. 6. Some nonlithogenic indicators from the trap samples including (a) total organic carbon (TOC) and (b) the foraminiferal concentration. The shaded rectangle indicates the likely period of typhoon influence. The significant wave height was recorded on the tripod.

temporal patterns corresponding to the typhoon. At the upper level, the abundance of both the planktonic and benthic species dropped off quickly to the pre-typhoon level 5 days after the time of the typhoon peak. However, at the lower level, the abundance of both foram types remained high, and tapered off gradually, resembling the pattern of the wet-sieved coarse fraction abundance (Fig. 8(b) in Liu and Lin, 2004).

The concentrations of foraminiferal shells in collecting cups at 54 and 104 m above the sea floor are not high (maximum 9 shells/g of dry weight). However, they are comparable to the concentrations in sediments on the sea floor along the canyon and adjacent shelf, which are less than 20 benthic shells per gram of sediment dry weight (Chiang et al., 2004). Furthermore, in another related study the same taxa of benthic foraminifers were also identified in stained coretop sediment samples (i.e., living shells) across the shelf and slope (Lin et al., in press) around the Kao-ping Submarine Canyon. This implies the resuspension of the distal substrate into the water column outside the canyon followed by shoreward and upcanyon transport. Episodic increases of planktonic foraminiferal fluxes in sediment-traps have also been reported on the shelf break and upper slope of the Middle Atlantic Bight in comparable water depths as a result of storm-related resuspension and transport of particles from the shelf to the upper slope (Brunner and Biscaye, 2003).

5.1.5. $\delta^{13}\text{C}$ of organic particles and the estimate of mixing factor (F_t)

The organic particles in the upper trap samples are generally ‘heavier’ and those in the lower trap are generally ‘lighter’ in terms of $\delta^{13}\text{C}$ (Fig. 7(a)). In fact, the estimated F_t values for the lower trap samples are mostly greater than 0.6, which is higher than those in the upper trap samples (Fig. 7(b)). This indicates that the particles in the lower trap had stronger terrestrial signals than particles 50 m above. Conversely, the particles captured by the upper trap have stronger marine signals, which are further enhanced during the period of typhoon influence (data points at 7/01 20:00 and 1/04 08:00).

5.2. Year 2002 experiment and typhoon Nakri

5.2.1. Fluvial and shelf processes

During the period of the 2002 deployments, both Typhoon Rammasun and Typhoon Nakri were present in the atmospheric pressure and coastal wind field records (Fig. 8(a)). Because of the remote distance of Rammasun (Fig. 3), it had little influence on the river discharge and the sea state in the study area (Figs. 8(a) and (b)).

There were two discharge events recorded at the gauging station (Fig. 8(b)). The one on July 12 is clearly related to Nakri, having peak river discharge of $2000\text{ m}^3/\text{s}$ and suspended sediment content about 550 mg/l . Corresponding to this event, the measured

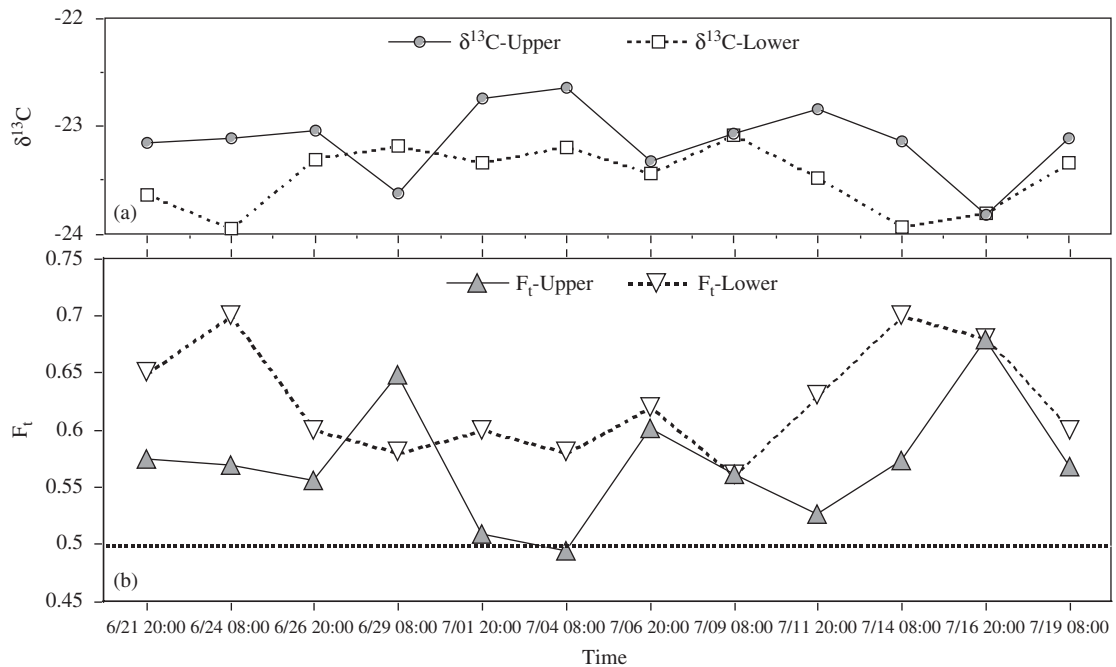


Fig. 7. Measured ^{13}C from the trap samples (a) and the estimated F_t (b).

SSC on the tripod seaward of the river mouth exceeded 30 mg/l (Fig. 8(b)).

Corresponding to the Nakri-related river discharge signal, the current measured at about 1 mab near the river mouth shows strong seaward flow (Fig. 8(c)). The seaward instantaneous flux of suspended sediment at the tripod site was then computed by the multiplication of measured SSC (Fig. 8(b)) and the seaward component of the flow (Fig. 8(c)). It is apparent that Nakri was a significant event for the export of suspended fluvial sediments (Fig. 8(d)).

The most visible coastal response to Nakri is the increased wave height exceeding 500 cm and increased peak period of incident waves exceeding 9 s (Fig. 8(e)). The passage of Nakri also coincided with the spring tide (Fig. 8(e)).

It is unfortunate that the ADCP deployed on the shelf was overturned on July 9, just before the effect of Nakri would have been recorded. Because of the selection criterion for good data, only 4 bins produced useful data, of which the flows at 2.4 and 5.4 mab are presented as progressive vectors (Fig. 9(a)). Although the flow pattern resembles that of the 2000 data, the influence of the wind field is readily noticeable as indicated by the small 'kink' (flow reversal) at July 3 and 4 on the 2.4 mab record,

which corresponds to the sudden shift of wind direction associated with Typhoon Rammasun on 14:00 July 3 (Fig. 8(a)). The offshore veering of the flow at 5.4 mab after July 4 is probably due to the downwelling-favorable winds following the onset of Rammasun.

5.2.2. Canyon processes

The observed current at 33 mab in the canyon shows the same pattern as the flow measured at 50 mab in 2000 in which the net upcanyon flow is superimposed by tidal oscillations at largely semidiurnal frequencies (Fig. 9(b)). The influence of Nakri on the near bottom flow in the canyon is not clear at this point. Additionally, the along-canyon flow at 33 mab has characteristics similar to those described by Liu and Lin (2004). Tidal motions at the M_2 frequency, having the major axis amplitude of 25.4 cm/s, dominate the flow field (Fig. 10(a)). The tidal energy accounts for 71% of the total energy in the along-canyon flow field.

The temporal fluctuations in the observed volume concentration of clay, very-fine-to-medium-silt, coarse-silt, and sand-sized suspended particles at 28 mab in the canyon were dominated by subtidal frequencies and tidal frequencies at diurnal and

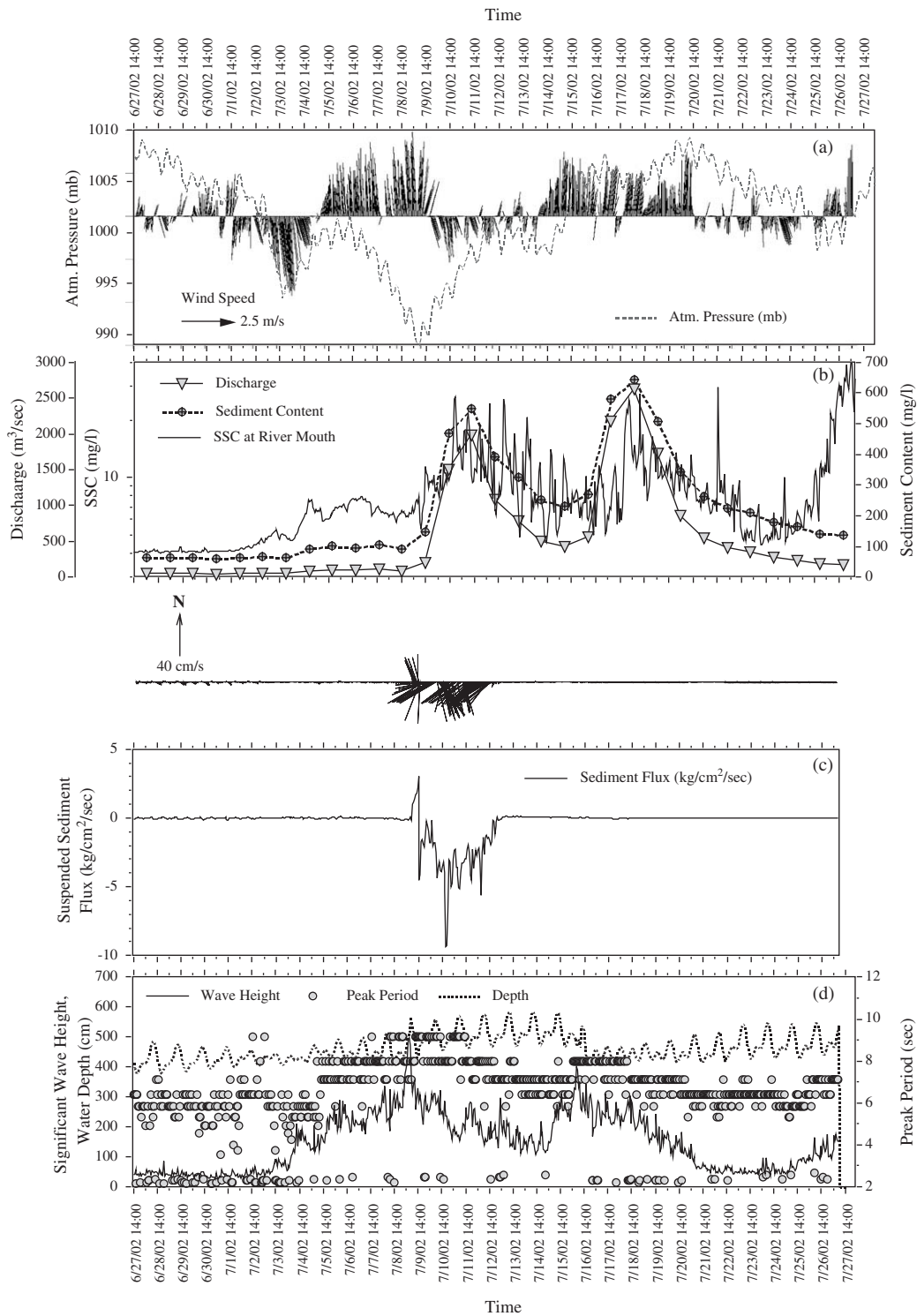


Fig. 8. Records of (a) coastal wind vectors (North direction is the top of the frame) plotted according to the oceanographic convention and the atmospheric pressure observed near the mouth of Kao-ping River, (b) daily river discharge and sediment content observed at the nearest gauging station and the SSC observed on the tripod at approximately 1 mab seaward of the mouth of KPR (Fig. 1), (c) the vector plot of the flow measured on the tripod approximately 1 mab seaward of the river mouth, and (d) the estimated instantaneous suspended sediment flux at 1 mab seaward of the river mouth, and (e) the significant wave height, peak wave period, and the water depth observed on the tripod between June 27 and July 27, 2002.

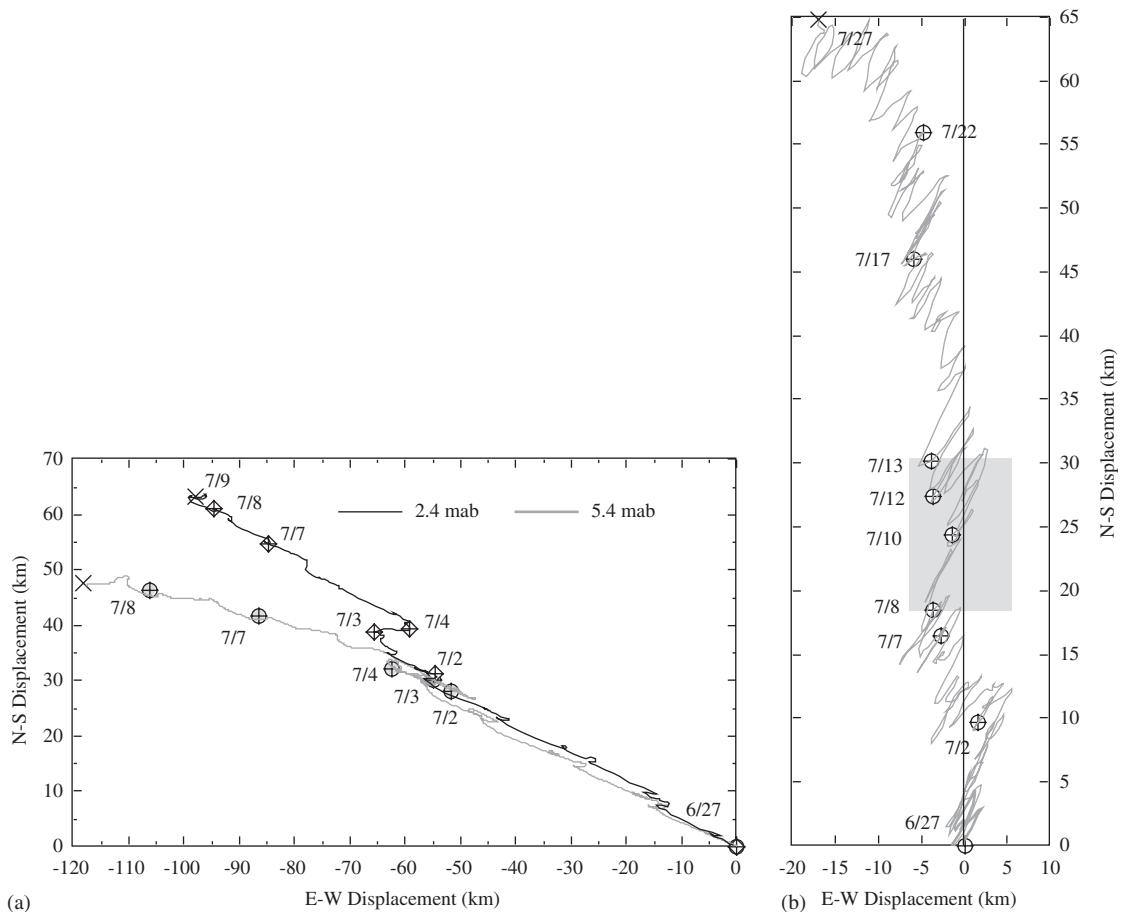


Fig. 9. Progressive vector plot of the flow measured by the (a) ADCP on the shelf from 00:00 June 28 to 04:00 July 7, and (b) remaining current meter approximately 33 mab in the canyon from 12:00 June 27 to 11:00 July 27. Selected time points are annotated on each record. The shaded box indicates the passing of Nakri. The origin of each plot is the beginning of the record and the cross represents the end of the record.

semi-diurnal bands (Fig. 10(b)). However, during the period of typhoon influence between July 8 and 14, the volume concentration increased by one order of magnitude for all four size-classes. These increases correspond closely to the same pattern in the SSC observed near the river mouth on the shelf. The close coupling is caused by the effect that the peak of river suspended sediment flux during Nakri coincided with offshore-directed winds (Figs. 8(a) and (d)), which is demonstrated by Liu and Lin (2004) in the case of Typhoon Kai-tak to facilitate downcanyon transport. It is worthwhile to note that the short duration of significant typhoon impact on the measured suspended particle concentrations in the canyon coincides with the neap-to-spring tidal phase (Fig. 10(b)), which implies that tide probably were not an important factor.

When comparing the temporal variations of the along-canyon flow and the volume concentrations of the suspended particles, one can see, during the period of typhoon influence, peak values of volume concentrations coincided with the maximum ebb current (Fig. 11). This leads to greater instantaneous downcanyon fluxes than the upcanyon fluxes of the four size-classes (Fig. 11(a)). Consequently, cumulative volume transport $Q(t)$ was estimated as

$$Q(t) = Q(t-1) + C(t)U(t)dt \quad (2)$$

(where $C(t)$ and $U(t)$ are the instantaneous volume concentration and the current velocity, respectively, and dt is the time increment) to indicate the trend of net particle movements (Fig. 11(b)). Before the onset of the typhoon, the cumulative transports of the four size-classes were near zero, suggesting little

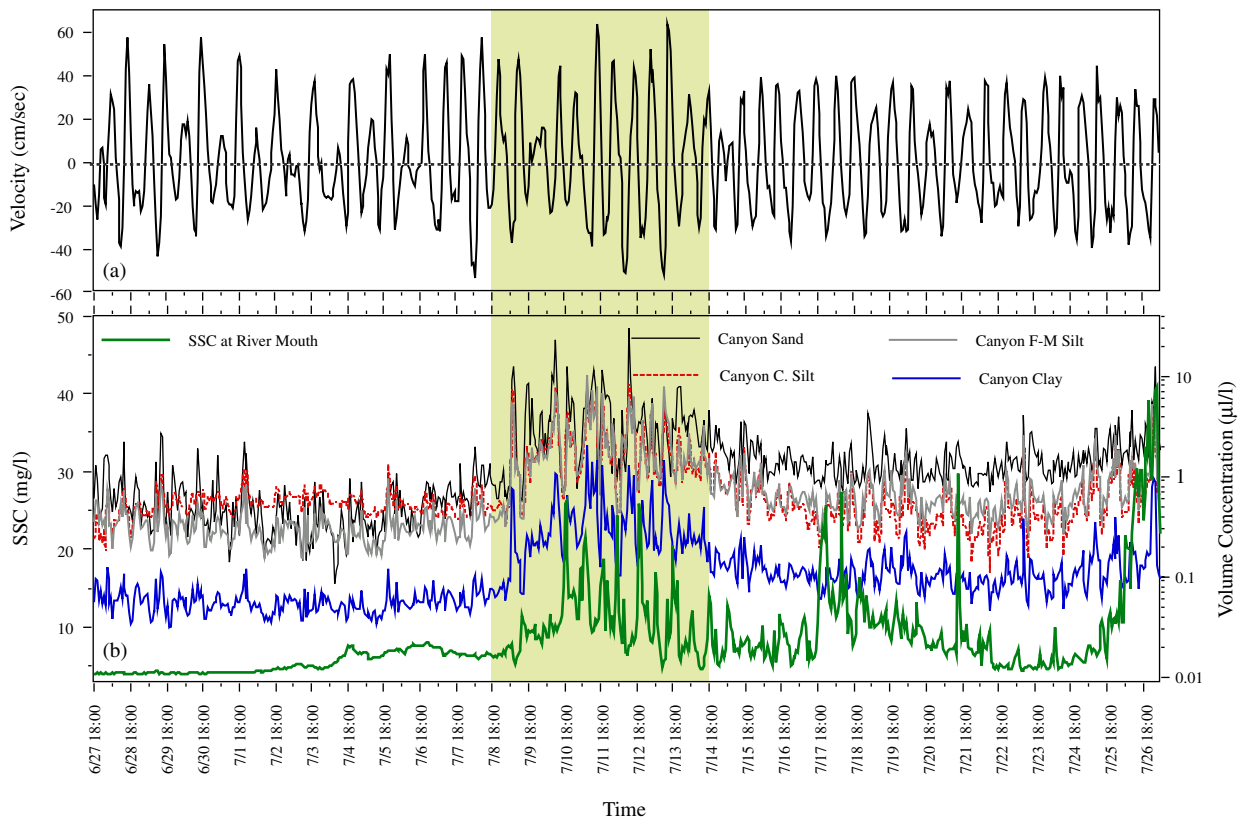


Fig. 10. Synoptic records of (a) the along-canyon component of the flow at 33 mab in the canyon and (b) the volume concentrations of clay-sized, very-fine-to-medium-silt-sized, coarse-silt-sized, and sand-sized suspended particles at 28 mab in canyon measured by LISST and the SSC measured on the tripod near the river mouth.

net transport up or down the canyon (Fig. 11(b)). During the period of typhoon influence, the net transports turned downcanyon as indicated by the negative slopes of the net transport curves. Yet, when the impact of the typhoon subsided, the net transports returned to the pre-typhoon pattern, as indicated by the near-horizontal orientation of the curves.

6. Discussion and conclusion

6.1. Two-way submarine conduit

6.1.1. Movements of water masses

The T–S diagram from the hydrographic profiling data (Fig. 12) at the reference station (Fig. 1) located at the opening of the head region of the canyon suggests that in addition to the effluent from KPR (Liu et al., 2002) the canyon is filled with two other types of water, the SCS water and the Kuroshio water. Generally, in the shallow part of

the canyon, the T–S characteristics suggest mixing between the three. However, in the deeper part of the canyon (temperature lower than 14 °C), the T–S diagram follows the signature of the SCS water exclusively (Fig. 12). Additionally, the flow measurements near the canyon floor in both years (2000 at 50 mab and 2002 at 33 mab) show net upcanyon flow, further supporting the possibility of intrusion of SCS water into the canyon. Although the current data series measured on the shelf in both years are short, they nevertheless show consistently net northwestward net flow, which could be from a branch of the Kuroshio.

6.1.2. Movements of suspended particles

Previously, Liu et al. (2002) used several statistical analyses of surficial sediment patterns to point out that both upcanyon and downcanyon sediment transport directions exist. Yet, the upcanyon direction is the dominant direction. Current measurements in 2000 indicate the net flow at the upper

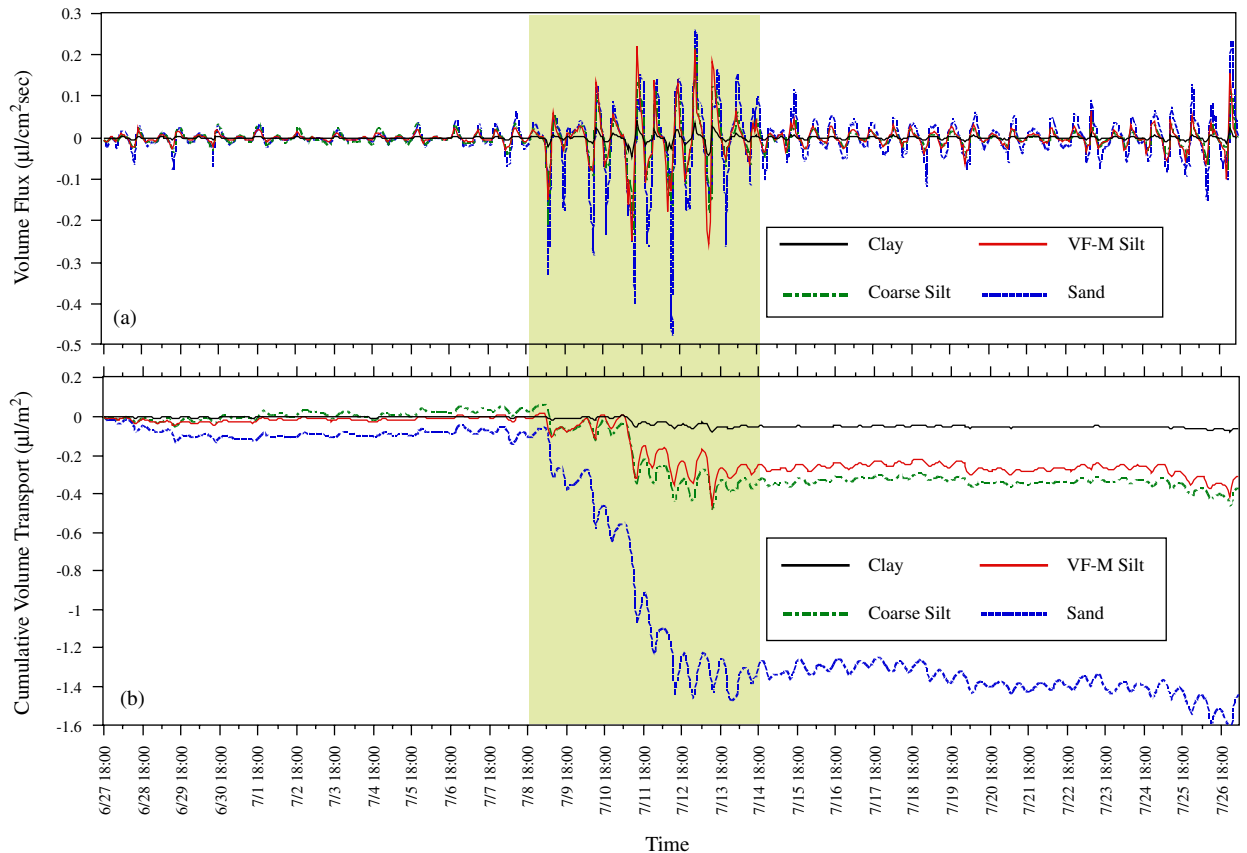


Fig. 11. The instantaneous volume flux of clay-sized, very-fine-to-medium-silt-sized, coarse-silt-sized, and sand-sized suspended particles (a) and their cumulative volume transport near the canyon floor (b). Positive values on both vertical axes represent upcanyon direction. The shaded area indicates the period of enhanced typhoon influence.

sediment-trap level is downcanyon and that at the lower trap level is upcanyon, so it would be reasonable to assume that the flow at 100 mab carries suspended particles downcanyon whereas the flow at 50 mab carries suspended particles upcanyon. The intrusion of the SCS water along the canyon floor can explain the presence of some benthic foram species in the sediment-traps whose nearest habitat should be in the northern part of the SCS.

Liu and Lin (2004) used 1-month measurements of particle volume concentrations and the flow in the lower part of the canyon to further point out that although tidal oscillations are strong, the net transport of suspended particles is upcanyon near the canyon floor. However, in this study using the same types of instruments located at similar depths and location in the canyon show net downcanyon transport of suspended particles (Fig. 11(b)). Although typhoon events occurred during both

one-month observations in 2000 and 2002, the typhoon in 2002 triggered a catastrophic transport episode that causes irreversible net downcanyon sediment transport. This suggests that tidal processes generally cause a net upcanyon sediment transport in the lower part of the canyon, yet episodic energetic events such as Typhoon Nakri could upset this pattern and result in net downcanyon transport pattern.

6.2. The effect of a typhoon on the delivery of terrestrial (proximal) and marine (distal) particles

There are some fundamental geographic differences between Kai-tak and Nakri that have significant bearing on how they impacted the study area. Kai-tak initially appeared in Bashi Channel hundreds of kilometers from the study area. It moved northward toward the study area and then moved away. Nakri on the other hand, became a

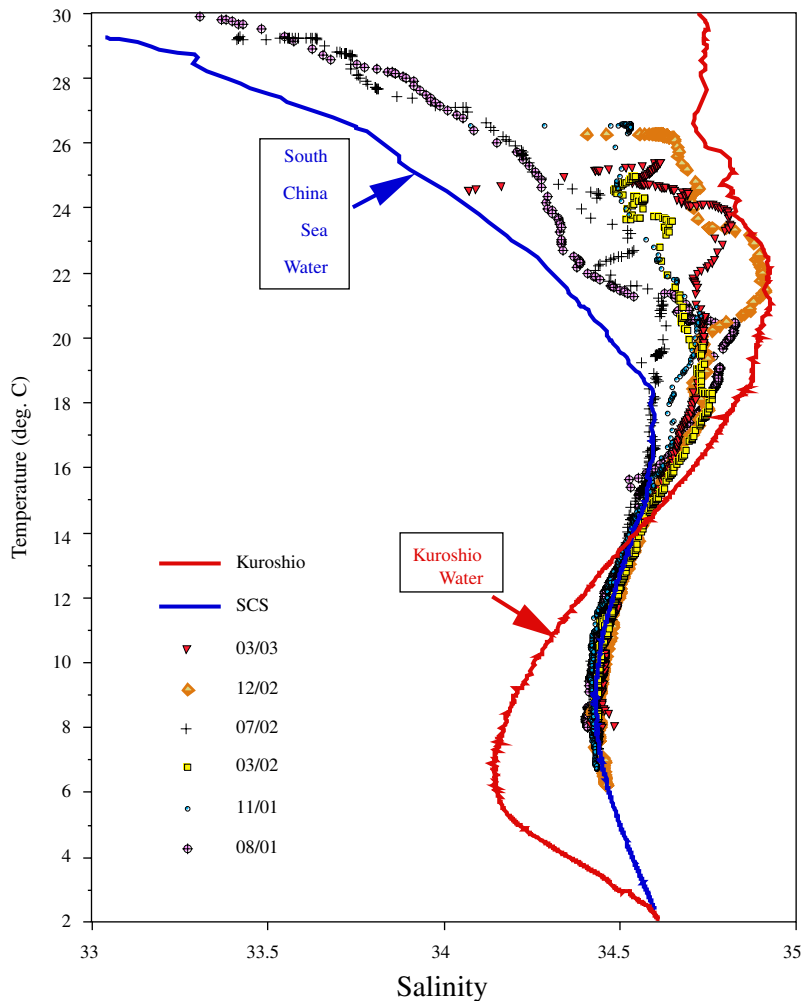


Fig. 12. T–S diagram from data collected at the reference hydrographic station shown in Fig. 1(b) and representative curves of the South China Sea (from observations in northern part of the SCS) water and Kuroshio water (from observations off southeastern Taiwan in the path of Kuroshio).

typhoon in southern Taiwan Strait at about 150 km directly due west of the study area moved north-eastward away from the study area and made landfall within about one day after its inception (Fig. 3).

To further aid in the ensuing discussions on the effect of the typhoon, it is helpful to establish the timelines of events during both Kai-tak (Table 1) and Nakri (Table 2) based on all the available data. In the case of Kai-tak in 2000, the sequence of occurrence of typhoon-related effects in the study area could be grouped into two phases: (a) A distal phase began with the presence of nonlithogenic signals of distal and marine origin in the submarine canyon (Table 1) probably due to the circulations generated by the typhoon while its center was still

hundreds of kilometers away from the study area (Fig. 3). (b) A proximal phase followed when the typhoon moved closer to the study area and the strengthened wind and wave fields had immediate impact on the study area. Typhoon-related episodic river discharge took place in this phase.

In another parallel study, stable isotope analyses were done on some of the sediment-trap samples in 2000 (Lin et al., in press). Oxygen isotopic compositions ($\delta^{18}\text{O}$) extracted from the carbonate foraminiferal shells usually bear information regarding the surrounding hydrography (Bemis et al., 1998; Imbrie et al., 1992; Linsley, 1996). From $\delta^{18}\text{O}$ of benthic forams in the coretop samples collected at a water depth about 1000 m in the South China Sea and of those collected in the sediment-trap

Table 2
Chronology of Typhoon Nakri related events in 2002

Timeline	Event	Phase
14:00 7/7	1. Onset of longer (9 s) waves (Fig. 8(e))	Distal
02:00 7/9	2. Lowest point of the atmospheric pressure (Fig. 8(a))	Proximal
02:00 7/9	3. Peak of significant wave height (Fig. 8(e))	Proximal
02:00 7/9	4. Onset of increased near-bottom flow at the river mouth (Fig. 8(c))	Proximal
06:00 7/9	5. Onset of increased suspended particle concentration near the canyon floor (Fig. 8(b))	Proximal
06:00 7/9	6. First enhanced peak of suspended particle fluxes near the canyon floor (Fig. 11(a))	Proximal
14:00 7/9	7. Abrupt change of wind direction (Fig. 8(a))	Proximal
14:00 7/10	8. Peak of the seaward suspended sediment flux at the river mouth (Fig. 8(d))	Proximal
02:00 7/11	9. Onset of high near-bed SSC at the river mouth (Fig. 8(b))	Proximal
14:00 7/11	10. Peak values of daily river discharge and sediment content (Fig. 8(b))	Proximal

Note: The accuracy of each timeline is to the nearest tick mark on the corresponding figure.

samples in 2000, Lin (2003) concluded that those benthic shells caught in the sediment-traps during the typhoon were transported from distal source areas of deeper water in the SCS.

It is unfortunate that no bio-geochemical data was available for Nakri; the sequence of its influence could be based only on physical forcings and responses. Because of the close proximity of this typhoon to the study area, the local responses are stronger; for example, the observed significant wave height exceeded 5 m (Fig. 8(e)) compared to 2.5 m in the case of Kai-tak (Fig. 6(a)). Because of the difference in the typhoons' relative positions along their tracks, the duration of impact was about 6 days for Kai-tak and about 4 days for Nakri (Tables 1 and 2). Another important difference to note is that Kai-tak was a medium-category typhoon (wind speed between 32.7 and 50.9 m/s near the center) and Nakri was a weak-category typhoon (wind speed between 17.2 and 32.5 m/s near the center).

Liu and Lin (2004) point out that the immediate influence of Kai-tak is the increased supply of reworked sediment on the shelf by wave resuspension. Yet, because of the landward winds during the typhoon, the related river discharge event did not create corresponding signals in the particle concentrations near the canyon floor. The wind effect is also demonstrated in the 2002 data set. Immediately after the passing of the eye of Nakri, the winds turned seaward coinciding with the typhoon-related river flux event (Fig. 8(d)). Consequently, there is a high correspondence between the measured SSC at the river mouth and the volume concentrations near the canyon floor during this period (Fig. 10(b)).

However, because of the landward winds corresponding to the second discharge event between July 16 and 20, no corresponding enhanced signals in the canyon were recorded (Figs. 8(a) and 10(b)).

Typhoon-related local processes such as coastal wind speed and direction, increased river discharge (proximal source) and wave resuspension (shelf processes and proximal source) contribute to the increased supply of both lithogenic (clastic) and nonlithogenic particles of terrestrial origin to the canyon (Liu and Lin, 2004). This fits the oceanic flood scenario described by Wheatcroft (2000). However, typhoons also enhance signals of marine particles as evidenced by the abrupt increase of foram concentration (Fig. 6(b)) and reduced terrestrial signals (Fig. 7(b)) as terrestrial particles are diluted by older and marine particles (Figs. 6(a) and (b)). Since typhoons (storms) are often formed in the distal ocean and move toward the river-sea system of interest, we therefore propose to expand the original concept of oceanic flood to include a distal phase in which the contribution of distal marine sources to a river-sea system occurs and a proximal phase in which locally generated sources dominate the input.

Another important point to note is in 2000, the mass fluxes (Fig. 5(b)) in the canyon remained high after the passing of spring tide, after all the observed distal (Figs. 6 and 7) and proximal influences (Fig. 6(a), Liu and Lin, 2004) of the typhoon had died out. This is speculated to be caused by distal sources brought to the study area by the circulations and swell associated with the wake of Kai-tak. Unfortunately, since the collecting cups were filled, the signals of later inputs were probably not

recorded, and this speculation could not be substantiated by the existing data.

6.3. Typhoon flushing-trigger for momentary downcanyon net transport

Because of the increased supply of terrestrial sediment by the river, reworked shelf sediment, and biogenic marine particles to the canyon during the typhoon, one would assume that a typhoon event would be an episode of increased deposition in the canyon. However, this might not be the case at the location of our sediment-trap array in the 2002 experiment. Although the net water movement near the canyon floor was upcanyon during the 2002 experiment (Fig. 9(b)), it was the co-oscillation between the observed volume concentrations and the along-canyon flow that determined the direction of net particle transport. Typhoon Nakri generated a short episode of increased fluxes, which was caused by primarily the increased particle volume concentration (Figs. 10(b) and 11(a)). Close examination of the fluctuations of particle volume concentration and the along-canyon flow reveals that during the typhoon most concentration peaks occur at the maximum downcanyon flow (Figs. 10(a) and (b)). Consequently, the downcanyon instantaneous fluxes exceed the upcanyon fluxes (Fig. 10), leading to net downcanyon transport (Fig. 11(b)).

In the case of Nakri, it is reasonable to assume that if there were no typhoon, the net particle transport would have been near zero (for clay and very-fine-to-medium-silt) to weakly upcanyon (for coarse-silt) and to weakly downcanyon (sand-sized particles). The episodic typhoon event not only creates an episode of strong transport equivalent to downcanyon flushing of all suspended particles but also set the net particle transport pattern to be downcanyon for the rest of the experiment period. On the surface, there are two essential elements in this downcanyon flushing mechanism, the abrupt increase of the supply of terrestrial sediment (magnitude) and the timing of the appearance of these particles near the canyon floor (phasing with the flow). In reality, many physical processes are involved including the interplay between the coastal wind field and river plume dynamics, shelf processes of waves and tides, canyon processes of stratification and internal tides, and the settling process of the particles themselves.

Because of this momentary flushing at the sediment-trap array location near the canyon floor, no deposits should be expected to form during this event. However, one can speculate that this flushing might trigger some kind of turbidity current or mass flow (Xu et al., 2004) along the canyon floor at some distance downcanyon, and the materials flushed downcanyon have to come to rest at some place, forming turbiditic deposits (Mulder et al., 2001). This is in fact a subject of on-going investigation of the strata of the canyon floor.

It is also important to note that this flushing mechanism was not observed during Kai-tak in the 2000 experiment using similar instrumentation and deployment design. There are many variables between the two typhoons that are not discussed in this paper such as the meteorological, oceanographic, and hydrological influences at regional and local scales on the submarine conduit. Furthermore, the spatial variability of the submarine canyon under the typhoon influence is not addressed in this paper. Therefore, although we have shown that the flushing mechanism reported in this paper is a significant form of typhoon influence, other forms of evidence might also exist.

Acknowledgements

The funding for this study was provided by the R.O.C. National Science Council under grant numbers NSC 91-2611-M-110-017 and NSC 92-2611-M-110-012 to J.T. Liu, NSC 91-2611-M-110-015-ODP to H.-L. Lin, and NSC 91-2621-Z-110-003 to J.-J. Hung. We want to express our sincere gratitude to Dr. Guo-wei Hung and his associates at the Sediment Trap Laboratory of the National Center for Ocean Research for their hard work in the design, assembly, deployment, and retrieval of the sediment-trap array. We are grateful to Peter Tsao's invaluable assistance in the field with the chartered boat operations and guarding the deployed instruments during the field experiment periods. We thank Captain Wu and his officers and crew of R/V Ocean Researcher III for their assistance in the data acquisition. We also thank Jeff C. Huang, Ray T. Hsu, Fanta Hsu, W.-C. Wang and I.-J. Lai for their help in the fieldwork and sample analysis. The Water Resources Bureau provided the hydrology data of Kao-ping River, and the Central Weather Bureau provided the weather data. Helpful comments and suggestions from two anonymous reviewers, John Milliman,

and Mike Bacon to improve the manuscript are gratefully acknowledged. Marilyn Ritzer-Liu proof-read a later version of the manuscript.

References

- Bemis, B.E., Spero, H.J., Bijma, J., Lea, D.W., 1998. Reevaluation of the oxygen isotopic composition of planktonic foraminifera: Experimental results and revised paleotemperature equations. *Paleoceanography* 13, 150–160.
- Brunner, C.A., Biscaye, P.E., 2003. Production and resuspension of planktonic foraminifers at the shelf break of the Southern Middle Atlantic Bight. *Deep-Sea Research I* 50, 247–268.
- Chiang, A.-P., Lin, H.-L., Lin, T.-C., 2004. Living (rose bengal stained) benthic foraminifera in sediments off the southwest Taiwan. In: *Proceedings of Fifth International Conference on Asian Marine Geology*, Bangkok, Thailand.
- Chung, Y., Chang, H.C., Hung, G.W., 2004. Particulate flux and ²¹⁰Pb determined on the sediment-trap and core samples from the northern South China Sea. *Continental Shelf Research* 24, 673–691.
- Craig, H., 1953. The geochemistry of the stable carbon isotopes. *Geochimica Cosmochimica Acta* 3, 53–92.
- Dadson, S.J., Novius, N., Chen, H., Dade, B.W., Hsieh, M.-L., Willet, S.D., Hu, J.-C., Horng, M.-J., Chen, M.-C., Stark, C.P., Lague, D., Lin, J.-C., 2003. Links between erosion, runoff variability and seismicity in the Taiwan orogen. *Nature* 426, 648–651.
- Fan, S., Swift, D.J.P., Traykovski, P., Bentley, S., Borgeld, J.C., Reed, C.W., Niedoroda, A.W., 2004. River flooding, storm resuspension, and event stratigraphy on the northern California shelf: observations compared with simulations. *Marine Geology* 210, 17–41.
- Harris, C.K., Butman, B., Traykovski, P., 2003. Winter-time circulation and sediment transport in the Hudson Shelf Valley. *Continental Shelf Research* 23, 801–820.
- Hsu, S.-C., Lin, F.-J., Jeng, W.-L., Chung, Y.-C., Shaw, L.-M., Hung, G.-W., 2004. Observed sediment fluxes in the southwestern most Okinawa Trough enhanced by episodic events: flood runoff from Taiwan rivers and large earthquakes. *Deep-Sea Research I* 51, 979–997.
- Hung, J.-J., Yang, C.-Y., Lai, I.-J., 2004. Meteorologic control on physical and chemical weathering rates and material fluxes from a tropical (Kaoping) river watershed in Taiwan. *Joint AOGS 1st Annual Meeting & 2nd APHW Conference*, Singapore, p. 759.
- Imbrie, J., Boyle, E.A., Clements, S.C., 1992. On the structure and origin of major glaciation cycles. 1. Linear responses to Milankovitch forcing. *Paleoceanography* 7, 701–738.
- Lin, H.-L., 2003. Late Quaternary deep-water circulation in the South China Sea. *Terrestrial Atmospheric and Oceanic Sciences* 14, 321–333.
- Lin, H.-L., Liu, J.T., G.-W. Hung. Foraminiferal shells in sediment-traps: implications of biogenic particle transport in the Kao-ping Submarine Canyon, in press.
- Linsley, B.K., 1996. Oxygen-isotope record of sea level and climate variations in the Sulu Sea over the past 150,000 years. *Nature* 380, 234–237.
- Liu, J.T., Lin, H.-L., 2004. Sediment dynamics in a submarine canyon: a case of river-sea interaction. *Marine Geology* 207, 55–81.
- Liu, C.-S., Huang, I.L., Teng, L.S., 1997. Structural features off southeastern Taiwan. *Marine Geology* 137, 305–309.
- Liu, J.T., Liu, K.-J., Huang, J.C., 2002. The influence of a submarine canyon on river sediment dispersal and inner shelf sediment movements: a perspective from grain-size distributions. *Marine Geology* 181 (4), 357–386.
- Mulder, T., Weber, O., Anschutz, P., Jorissen, F.J., 2001. A few months-old storm-generated turbidite deposited in the Capbreton Canyon (Bay of Biscay, SW France). *Geo-Marine Letters* 21, 149–156.
- Ogston, A.S., Cacchione, D.A., Sternberg, R.W., Kineke, G.C., 2000. Observation of storm and river flood-driven sediment transport on the northern California continental shelf. *Continental Shelf Research* 20, 2141–2162.
- Perterson, B.J., Howarth, R.W., 1987. Sulfur, carbon, and nitrogen isotopes used to trace organic matter flow in the salt-marsh estuaries of Sapelo Island, Georgia. *Limnology and Oceanography* 32, 1195–1213.
- Puig, P., Palanques, 1998. Temporal variability and composition of settling particle fluxes on the Barcelona continental margin (Northwestern Mediterranean). *Journal of Marine Research* 56, 639–645.
- Puig, P., Ogston, A.S., Mullenbach, B.L., Nittrouer, C.A., Sternberg, R.W., 2003. Shelf-to-canyon sediment transport processes on the Eel continental margin (northern California). *Marine Geology* 193, 129–149.
- Sheu, D.D., Jou, W.C., Chen, M.J., Lee, W.Y., Lin, S., 1995. Variations of calcium carbonate, organic carbon and their isotopic compositions in surface sediments of the East China Sea. *Terrestrial, Atmospheric and Oceanic Sciences* 6, 115–128.
- Skiris, N., Lacroix, Djenidi, S., 2004. Effects of extreme meteorological conditions on coastal dynamics near a submarine canyon. *Continental Shelf Research* 24, 1033–1045.
- Sobarzo, M., Figueroa, M., Djurfeldt, L., 2001. Upwelling of subsurface water into the rim of Biobio submarine canyon as a response to surface winds. *Continental Shelf Research* 21, 279–299.
- Tyson, R.V., 2001. Sedimentation rate, dilution, preservation and total organic carbon: some results of a modelling study. *Organic Geochemistry* 32, 333–339.
- Vitorino, J., Oliveira, A., Jouanneau, J.M., Drago, T., 2002. Winter dynamics on the northern Portuguese shelf. Part 2: bottom boundary layers and sediment dispersal. *Progress in Oceanography* 52, 155–170.
- Wheatcroft, R.A., 2000. Oceanic flood sedimentation: a new perspective. *Continental Shelf Research* 20, 2059–2066.
- Xu, J.P., Noble, M.A., Rosenfeld, L.K., 2004. In-situ measurements of velocity structure of turbidity currents in Monterey Submarine Canyon, California. *Geophysical Research Letters* 31, L0911.